



ELSEVIER

Contents lists available at ScienceDirect

Control Engineering Practice

journal homepage: www.elsevier.com/locate/conengprac

Zero-phase velocity tracking of vibratory systems

D.-W. Peng^{*}, T. Singh, M. Milano

Department of Mechanical and Aerospace Engineering, University at Buffalo, 318 Jarvis Hall, Buffalo, NY, USA

ARTICLE INFO

Article history:

Received 4 November 2013

Accepted 20 March 2015

Keywords:

Input shaping
Time delay filtering
Velocity tracking
Vibration control
Zero phase
Openloop control

ABSTRACT

The focus of this paper is on the development of an input shaper/time-delay filter that permits the precise tracking of a ramp input, while eliminating residual vibrations. Zero phase error velocity tracking is often required in applications where moving parts have to be mated, such as manufacturing lines with high production output. A closed form solution to a pre-filtering technique is presented which achieves the desired characteristics. The performance of this technique is compared with other input shaper designs in current literature, and is shown to achieve smaller settling time and maintain zero steady state phase error without a priori knowledge of the initiation and termination of ramp profiles. The technique is then physically applied to a rotary pendulum to demonstrate the consistency of its ramp tracking and vibration reduction capabilities.

© 2015 Elsevier Ltd. All rights reserved.

1. Introduction

Input shaping is a feedforward control technique that has been used extensively to eliminate residual vibrations for systems undergoing rest-to-rest maneuvers (Singer & Seering, 1990; Singh & Vadali, 1993a; Sorensen, Singhose, & Dickerson, 2007). This is achieved by convolving the reference step input with a sequence of impulses that cancel the oscillatory dynamics present in the target system. Additional impulses can be introduced into the sequence to improve robustness to uncertainties in the model parameters, at the cost of longer maneuver times. Various groups (Rhim & Book, 2004; Tzes & Yorkovich, 1993) have also developed adaptive input shaping schemes to improve the robustness while minimizing the duration of impulse sequence.

While traditional input shaping schemes have been well demonstrated for rest-to-rest maneuvers, there are instances where constant velocity tracking is required. Constant velocity motion is represented by a ramp signal, and the direct application of input shaping schemes introduces a non-zero steady state phase lag after the residual vibrations are eliminated. In some cases, this phase error is permitted as it does not interfere with operation requirements, such as in the control of high-speed electron microscopy scanner head (Croft & Devasia, 1999), wafer scanner (Butler, 2013), and high speed tape drives (Mathur & Messner, 1998). Masterson, Singhose, and Seering (2000) recognize the delay generated in completing a prescribed scan when an input shaper is used to eliminate residual vibrations. To satisfy the

constraint imposed by the scan time, they study the effect of changing the scan velocity to compensate for the delay. For applications where zero velocity tracking error is crucial to the operation, traditional input shapers are no longer sufficient. Such requirement arises when compliant industrial robots are used in high throughput production lines. Kamel, Lange, and Hirzinger (2008) discussed the need for zero phase error tracking during mating operations between car wheels and the corresponding chassis moving with constant velocity on an assembly line. The wheels are handled by robotic end-effectors with built-in compliance to avoid damaging the chassis. The same compliance also introduces oscillations that are detrimental to the alignment, and input shapers are used to minimize the vibrations.

Attempts to reduce or eliminate ramp tracking error have been suggested in Masterson et al. (2000), Tomizuka (1987), Butterworth, Pao, and Abramovitch (2008), and Kamel et al. (2008). Masterson et al. (2000) developed a procedure for constant velocity scanning with flexible sensors by increasing the reference scan velocity to compensate for the phase lag due to input shapers, while maintaining the total scan time. Tomizuka (1987) proposed a zero phase error tracking algorithm, which relies on a priori knowledge of the trajectory and is often referred to as a model inversion based technique. Butterworth et al. (2008) compared the performance of model inversion techniques on velocity tracking of an atomic force microscope which is characterized by non-minimum phase behavior. Dynamic inversion assuming an output with a desired smoothness permits identifying a bounded smooth input which has been shown to track a reference profile by Piazzi and Visioli for the end point control of a flexible link (Piazzi & Visioli, 2011) and for the control of an overhead crane (Piazzi & Visioli, 2002). Dynamic inversion has also been demonstrated to work well for nonlinear systems with affine input where the number of inputs and outputs is the same

^{*} Corresponding author.

E-mail addresses: dpeng2@buffalo.edu (D.-W. Peng), tsingh@buffalo.edu (T. Singh), mmilano@buffalo.edu (M. Milano).

(Devasia, Chen, & Paden, 1996). Kamel et al. (2008) described several methods for input shaping with predictive path scheduling for low sampled systems in their efforts to damp oscillations in the robot end effector. In all these cases, their designs are acausal and require knowledge of the maneuver trajectory.

In this paper, a simple casual technique consisting of a shaped ramp profile in conjunction with a shaped step profile is shown to achieve precise ramp signal tracking. Traditional input shaping schemes are readily applicable within the ramp-following framework, allowing for improvements in robustness, as well as designs for multi-mode systems in both the continuous and discrete domain. Closed-form solutions are also available, allowing for efficient implementations. Finally, the technique is applied to the velocity tracking of a rotary pendulum for experimental validation.

2. Time-delay filter/input shaper

Input shapers (IS) and time-delay filters (TDF) are pre-filtering techniques that are often used to eliminate residual vibrations in rest-to-rest maneuvers. The IS design is derived in the time-domain while the TDF is designed in the frequency domain. The terms IS and TDF are used interchangeably in this paper, and in figures they are labeled based on the employed design methods. Time-delay filter relies on canceling the under-damped poles of the system with zeros of the time-delay filter transfer function. This section will briefly review the results from traditional TDF design that are immediately applicable to the development of the ramp-following time delay filters (RF-TDF), the reader is referred to Singh (2010) for a more comprehensive treatment.

The general structure of a time-delay filter is shown in Fig. 1. Specifically for a second order under-damped system

$$G(s) = \frac{Y(s)}{U(s)} = \frac{\omega^2}{s^2 + 2\zeta\omega s + \omega^2}, \quad (1)$$

a minimum of two terms in the time-delay filter $P(s)$ is required to cancel the poles of the system. The single-delay TDF ($N=2$) therefore assumes the form

$$P(s) = \sum_{i=0}^{N-1} A_i e^{-sT_i} = A_0 + A_1 e^{-sT_1}, \quad (2)$$

which is set to zero at the system poles $s = -\zeta\omega + j\omega\sqrt{1-\zeta^2}$, to obtain a closed form solution for the parameters of the time-delay filter:

$$A_0 = \frac{e^{\zeta\pi/\sqrt{1-\zeta^2}}}{1 + e^{\zeta\pi/\sqrt{1-\zeta^2}}}, \quad A_1 = \frac{1}{1 + e^{\zeta\pi/\sqrt{1-\zeta^2}}}, \quad T = \frac{\pi}{\omega\sqrt{1-\zeta^2}}. \quad (3)$$

The resulting filter corresponds exactly to the solution of the posicast controller (Smith, 1957) and the zero-vibration (ZV) input shaper (Singer & Seering, 1990). The residual vibrations after the final maneuver time T_{N-1} is completely eliminated when the system parameters are known exactly. It is important to note that the DC gain of any time-delay filter must be unity, i.e.

$$\sum_{i=0}^{N-1} A_i = 1 \quad (4)$$

to ensure that the output amplitude is the same as the input amplitude of the step after the final maneuver time. Fig. 2 shows the response of a second order system to the filtered step input.

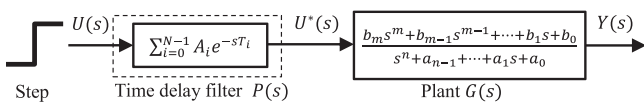


Fig. 1. Traditional time-delay filter structure.

2.1. Robust design (TDF)

The performance of the time-delay filter depends on the knowledge of the system model. Since the parameters of the system model are seldom known exactly in practice, there is a need to synthesize TDF that are insensitive to errors in these parameters.

2.1.1. Cascade design

Singh and Vadali (1993b) have shown that by placing multiple zeros of the time-delay filter at the nominal location of the uncertain poles of the system, one can achieve robustness in the proximity of the nominal model. For instance, by cascading two single TDF, the robust TDF with two delays is given as

$$P(s) = (A_0 + A_1 e^{-sT_1})^2 = A_0' + A_1' e^{-sT_1} + A_2' e^{-s2T_1} \quad (5)$$

where A_0 , A_1 and T_1 are the same as (2). Evidently from the above equation, the final maneuver time is now $2T_1$, i.e. the increase in robustness also increases the maneuver time. The formulation is equivalent to adding an additional constraint forcing the derivatives of the TDF at the nominal frequency or damping ratio to be also zero (Singh & Vadali, 1993b). This is sometimes referred to as zero vibration and derivative (ZVD) input shaper (Singer & Seering, 1990). Higher derivatives can also be forced to zero by cascading additional single-delay TDF, which further improves the robustness while increasing maneuver time. Larger maneuver time is often undesirable in high-speed precision applications, thus the trade-off between robustness and maneuver time must be carefully considered. For the remainder of this paper, the parameterization given by (5) will be simply referred to as the robust TDF.

2.1.2. Minimax design

TDF with 2 delays introduces robustness based on the knowledge of nominal model parameters. Alternatively, a minimax TDF can be designed to improve the robustness within a domain of uncertainty (Singh, 2010). Since the minimax TDF is a numerical optimization based technique, only a special case is considered here such that its applicability to the ramp-following time delay filter can be assessed in subsequent sections.

The minimax TDF is designed for the same second order system in (1) subjected to a unit step input. A uniform distribution for the uncertainty in the natural frequency is assumed. The optimization problem can be stated as

$$\min_{A_i, T_i} \max_{\omega} \frac{1}{2} y_f^2 + \frac{1}{2} \omega^2 (y_f - y_{ref})^2 \quad (6)$$

subject to the following constraints on the TDF parameters:

$$\sum_{i=0}^{N-1} A_i = 1 \quad (7)$$

$$0 < T_{i-1} < T_i, \quad (8)$$

where the subscript f denotes value of the variable immediately after the final maneuver time T_{N-1} . The cost function (6) measures the residual energy of the system response for normalized mass $m=1$, with corresponding stiffness ω^2 . The uncertain domain over ω is discretized to produce a set of plant models. A unit step input is shaped by the candidate time-delay filter, and the residual energy is evaluated for each plant model. The maximum residual energy over the specified range of uncertain ω is minimized, resulting in a desensitized time-delay filter design. A two-delay TDF ($N=3$) is used here, and the minimax problem is solved with MATLAB's `fminimax` function to obtain the parameters A_0 , A_1 , A_2 , T_1 and T_2 . While minimax design based on the present cost function has been shown to reduce residual vibrations effectively for rest-to-rest maneuvers (Singh, 2002), it will be illustrated in

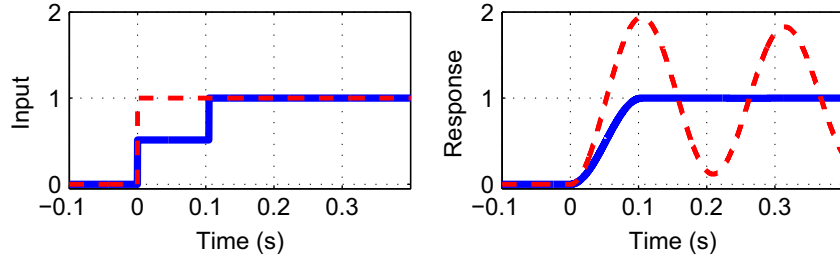


Fig. 2. Left: unfiltered step input (dash) and filtered step input (solid). Right: response of an underdamped second order system to step input (dash) and to the filtered input (solid).

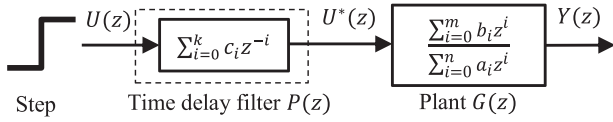


Fig. 3. Time-delay filter structure for discrete systems.

Section 5 that the minimax technique fails to achieve the goal of precise ramp tracking.

2.2. Multi-mode design (TDF)

TDF design techniques can be easily extended to higher order system. Consider the multiple-mode system in the form

$$G(s) = \prod_{k=1}^m \frac{G_{num,k}(s)}{s^2 + 2\zeta_k \omega_k s + \omega_k^2}, \quad (9)$$

with $2m$ complex poles located at $s = -\zeta_k \omega_k \pm j\omega_k \sqrt{1 - \zeta_k^2}$, $k = 1 \dots m$. $G_{num,k}(s)$ is the numerator for k th mode, under the constraint that the overall DC gain for $G(s)$ is unity. Then TDF's for single-mode systems can be cascaded to cancel the individual pole pairs in (9), i.e.

$$P(s) = \prod_{k=1}^m P_k(s) = \sum_{i=0}^{N-1} A_i e^{-sT_i}, \quad (10)$$

where $P_k(s)$ is the TDF designed for the k th mode. Either (2) or (5) can be used as $P_k(s)$ depending on the desired level of robustness. However, this procedure does not necessarily produce the smallest possible maneuver time for a given system. Concurrent design for multi-mode system shown in Singh (2010) can be used if minimal maneuver time is desired.

2.3. Discrete design (TDF)

The concepts of time-delay filter for continuous systems can be applied to discrete systems in the same fashion. Fig. 3 illustrates the structure of the TDF in the discrete domain. Consider the system of the form

$$G(z) = \frac{\sum_{i=0}^m b_i z^i}{\sum_{i=0}^n a_i z^i} \quad (11)$$

The discrete time-delay filter can be posed as the design of a FIR (finite impulse response) filter (Singh, 2010), i.e.

$$P(z) = \sum_{i=0}^k c_i z^{-i}, \quad (12)$$

which places k poles at the origin of the z -plane. The zeros of $P(z)$ can be selected by choosing appropriate c_i 's in order to cancel the poles of the system $G(z)$. To determine the parameters c_i for the FIR

filter, an optimization problem can be posed as follows:

$$\min_{c_i} J = \sum_{i=0}^k (i+1)^\lambda |c_i| \quad (13)$$

subject to

$$\operatorname{Re} \left[\sum_{i=0}^k c_i (\sigma_j + \omega_j \sqrt{-1})^{-i} \right] = 0 \quad \forall j = 1, 2, \dots, n$$

$$\operatorname{Im} \left[\sum_{i=0}^k c_i (\sigma_j + \omega_j \sqrt{-1})^{-i} \right] = 0 \quad \forall j = 1, 2, \dots, n$$

$$\sum_{i=0}^k c_i = 1$$

$$0 < c_i < 1 \quad \forall i = 1, 2, \dots, k \quad (14)$$

which will place $2n$ zeros at the nominal location of the poles of the system, i.e. $z_j = \sigma_j + \omega_j \sqrt{-1}$ (Only one root from each complex pair needs to be included in the constraints.). $(i+1)^\lambda$ is the weighting factor that increases the penalty non-linearly with time, where λ is chosen to be > 1 . Similar to the design of TDF in the continuous-time, robustness can be introduced by locating multiple zeros of the FIR filter at the estimated location of the poles of the system, which results in desensitizing the FIR filter to modeling errors. This can be accomplished by including additional constraints as follows:

$$\operatorname{Re} \left[\sum_{i=0}^k i c_i (\sigma_j + \omega_j \sqrt{-1})^{-i-1} \right] = 0 \quad \forall j = 1, 2, \dots, n$$

$$\operatorname{Im} \left[\sum_{i=0}^k i c_i (\sigma_j + \omega_j \sqrt{-1})^{-i-1} \right] = 0 \quad \forall j = 1, 2, \dots, n. \quad (15)$$

Since the pulses are discrete, the parameters c_i can be efficiently solved as a linear programming problem (Singh, 2010). The ability to handle multiple modes is implicit in this formulation.

3. Ramp-following TDF

Although time-delay filters are primarily used to eliminate residual vibrations due to step inputs, they are applicable for any kind of reference trajectories. When TDF is applied to a ramp input, the shaped signal is a series of changes in slopes, such that the final slope matches the slope of the original signal. The shaped ramp signal effectively eliminates residual vibrations. However, a phase lag is manifested between the steady state system response and the input ramp signal, as shown by the dotted line in Fig. 7(b). This issue leads to performance degradation when there is a need for zero-phase tracking error in precision applications. The design of a precise ramp-following time-delay filter (RF-TDF) therefore relies on the knowledge of the steady state ramp tracking error, which will be derived in this section.

First consider a general stable transfer function of the form

$$G(s) = \frac{b_m s^m + b_{m-1} s^{m-1} + \dots + b_1 s + b_0}{s^n + a_{n-1} s^{n-1} + \dots + a_1 s + a_0} \quad (16)$$

where $m < n$. Since TDF is an open loop control, the DC gain of the system itself must be unity to result in finite ramp tracking error, i.e.

$$b_0 = a_0. \quad (17)$$

For a ramp input, $U(s) = 1/s^2$, the steady state tracking error due to the system dynamics is

$$h_{\text{sys}} = \lim_{s \rightarrow 0} sU(s)(1 - G(s)) \quad (18)$$

$$h_{\text{sys}} = \frac{a_1 - b_1}{a_0} \quad (19)$$

When the time delay filter $P(s) = \sum_{i=0}^{N-1} A_i e^{-sT_i}$ is introduced, the steady state ramp tracking error h can be derived as follows:

$$h = \lim_{s \rightarrow 0} s \frac{1}{s^2} \left(1 - P(s) \frac{b_m s^m + \dots + b_1 s + b_0}{s^n + a_{n-1} s^{n-1} + \dots + a_1 s + a_0} \right) \quad (20)$$

$$h = \lim_{s \rightarrow 0} \left(\frac{s^n + a_{n-1} s^{n-1} + \dots + (a_m - b_m P(s)) s^m + \dots + (a_1 - b_1 P(s)) s}{s(s^n + a_{n-1} s^{n-1} + \dots + a_1 s + a_0)} \right) \quad (21)$$

$$+ \lim_{s \rightarrow 0} s \left(\frac{a_0 - b_0 P(s)}{s^n + a_{n-1} s^{n-1} + \dots + a_1 s + a_0} \right). \quad (22)$$

Recall (4) and (17), such that

$$\lim_{s \rightarrow 0} P(s) = \sum_{i=0}^{N-1} A_i = 1, \quad (23)$$

Therefore

$$h = h_{\text{sys}} + \lim_{s \rightarrow 0} s \frac{1}{s^n + a_{n-1} s^{n-1} + \dots + a_1 s + a_0} a_0 (1 - P(s)) \quad (24)$$

$$h = \frac{a_1 - b_1}{a_0} + \lim_{s \rightarrow 0} \frac{0}{s} \quad (25)$$

Using L'Hospital's rule on the second term, we have

$$\lim_{s \rightarrow 0} \frac{\frac{d}{ds} a_0 (1 - \sum_{i=0}^{N-1} A_i e^{-sT_i})}{\frac{d}{ds} s(s^n + a_{n-1} s^{n-1} + \dots + a_1 s + a_0)} = \sum_{i=0}^{N-1} A_i T_i, \quad (26)$$

which we define as h_{tdf} the tracking error attributed to the pre-filter. The steady state ramp tracking error due to the traditional TDF can be represented as

$$h = h_{\text{sys}} + h_{\text{tdf}} = \frac{a_1 - b_1}{a_0} + \sum_{i=0}^{N-1} A_i T_i. \quad (27)$$

Since prefiltering a ramp input through a time-delay filter designed to cancel the under-damped modes of the system results in a steady-state error, one can augment the reference input with a time-delay filtered step input of the size of the steady-state error. This should, after the execution of the final-delay, result in zero-error ramp following output profile.

A simple ramp-following time-delay filter can now be synthesized as shown in Fig. 4 by exploiting the knowledge of the steady state tracking error.

The first block in Fig. 4 splits the ramp signal into two terms to achieve precise ramp tracking capability: the first term with a gain

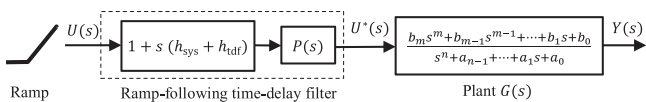


Fig. 4. Ramp-following time-delay filter structure.

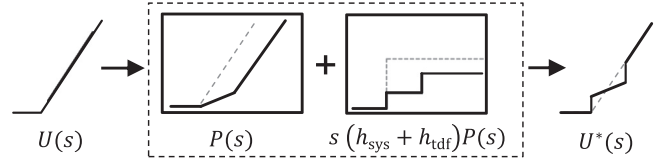


Fig. 5. The ramp-following time-delay filter at a glance.

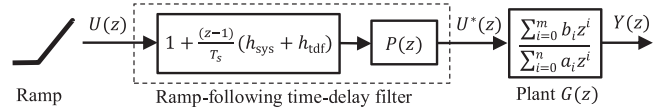


Fig. 6. Ramp-following time-delay filter structure for discrete systems. Note that a_n is assumed to be 1 for the formulation of h_{sys} and h_{tdf} in this paper.

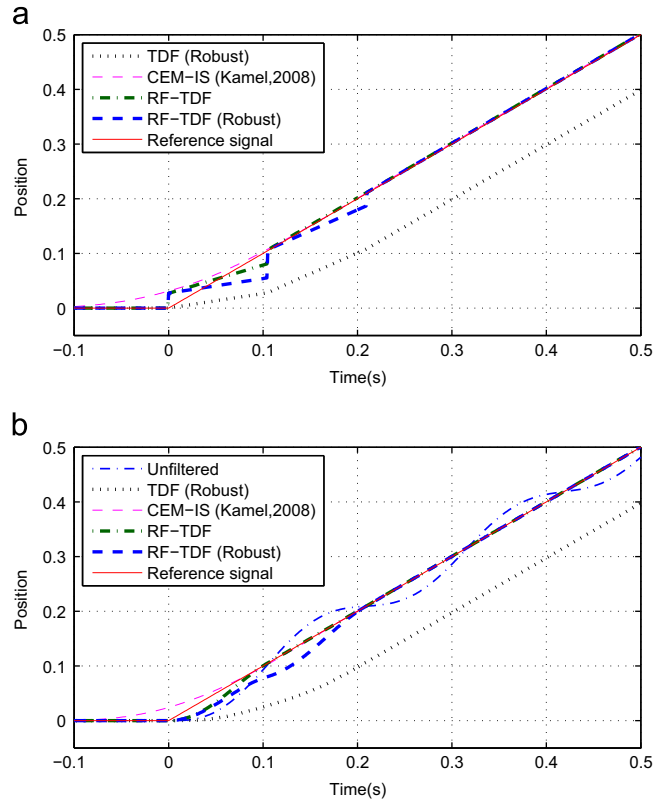


Fig. 7. Simulation results for a second order system with $\omega_n = 30$ rad/s and $\zeta = 0.02$. (a) Shaped ramp inputs. (b) Ramp responses.

of unity feeds through the ramp input, and the second term produces a step input with the derivative s . The step is scaled by $h = h_{\text{sys}} + h_{\text{tdf}}$ to compensate for the steady state ramp tracking error. Since both signals are subsequently modified to cancel the system poles at the sub-TDF stage $P(s)$, residual vibrations are eliminated when the model parameters are known exactly. The time-delay filter $P(s)$ can be chosen to be either (2) or (5), depending on the desired level of robustness. The idea behind RF-TDF is summarized in Fig. 5.

For a second order system in the form of (1), it can be easily shown that the steady state ramp tracking error reduces to

$$h = \frac{2\zeta}{\omega} + \sum_{i=0}^{N-1} A_i T_i \quad (28)$$

Kamel et al. (2008) have suggested adding the $2\zeta/\omega + \sum_{i=1}^{N-1} A_i T_i = 0$ term as a constraint in their optimization to produce

Table 1
Settling time to a unit ramp for various input shapers, with simulation step size $\Delta t = 0.001$ s.

Settling time (s)	
CEM-IS (Kamel et al., 2008)	0.254 ^a
RF-TDF	0.083
RF-TDF (Robust)	0.178

^a CEM-IS shifts the reference signal backwards in time to achieve precise ramp tracking, the settling time shown here includes the shifting time.

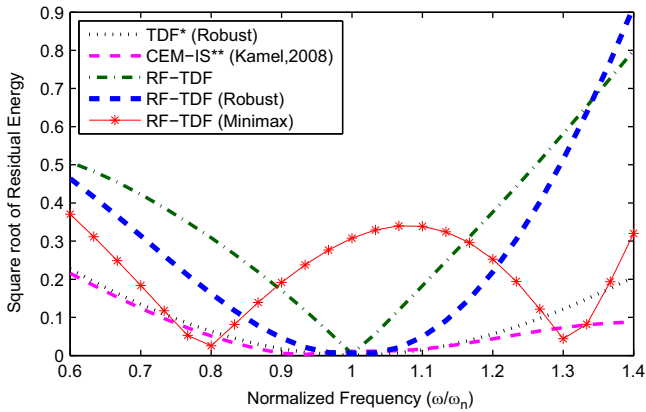


Fig. 8. Sensitivity of various input shaper for $0.6 < \omega/\omega_N < 1.4$. ω_N is the nominal frequency. *The curve for TDF has been biased to remove steady state tracking error. **CEM-IS uses backwards time shifting to eliminate the steady state tracking error.

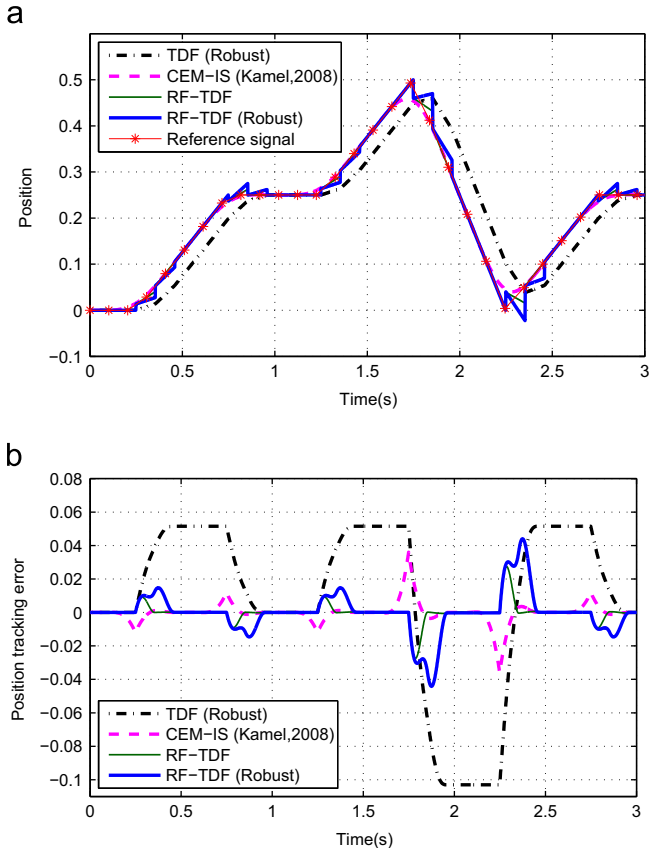


Fig. 9. Simulation results for a second order system with $\omega = 30$ rad/s and $\zeta = 0.02$. The signal profile is taken from Kamel et al. (2008). (a) Shaped input to a finite rate signal. (b) Reference signal tracking error.

Table 2
Average tracking error of input shapers to the reference signal in Fig. 9a.

Average tracking error	
TDF (Robust)	0.025072
CEM-IS (Kamel et al., 2008)	0.0032127
RF-TDF	0.0026052
RF-TDF (Robust)	0.0058716

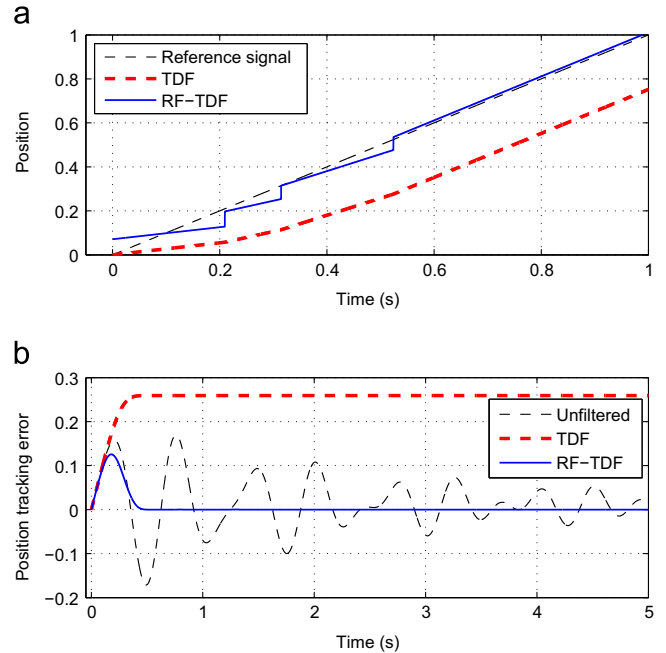


Fig. 10. Simulation for a system with multiple-modes subjected to ramp input. Note that the time axes are scaled differently. (a) Shaped input to a multi-mode system. (b) Reference signal tracking error.

input shaper parameters with zero ramp tracking error for a second order system. In essence, their approach attempts to account for the amplitude compensating step in Fig. 4 by using only the parameterization in Fig. 1. Constraining Eq. (28) results in negative value for some A_i which results in large positive values for the complementary A_i 's. Naturally, these steps manifest as large amplitudes within short sequences of impulses in their solution, making it difficult to provide initial optimization guesses and physically implement the input shaper.

3.1. Robust design (RF-TDF)

Since the ramp-following time-delay filter presented is simply a sum of filtered step and ramp inputs, typical methods employed to improve robustness in traditional time delay filters can be directly applied. Using the TDF parameters from (5) as the $P(s)$ term in Fig. 4 will desensitize the RF-TDF to uncertainties about nominal system parameters. This will be referred to as the robust RF-TDF for the remainder of this paper.

The minimax TDF design can also be used with the RF-TDF structure shown in Fig. 4. The TDF parameters in $P(s)$ are now the solutions to the optimization problem equation (6). As later sections will show, the minimax design in its present form is unsuitable in the context of RF-TDF due to the lackluster ramp tracking capabilities.

3.2. Discrete design (RF-TDF)

As in the case of continuous-time RF-TDF designs, classic TDF synthesized in the discrete domain, $P(z)$, can be directly applied as a part of the structure shown in Fig. 6 to allow for precise ramp signal

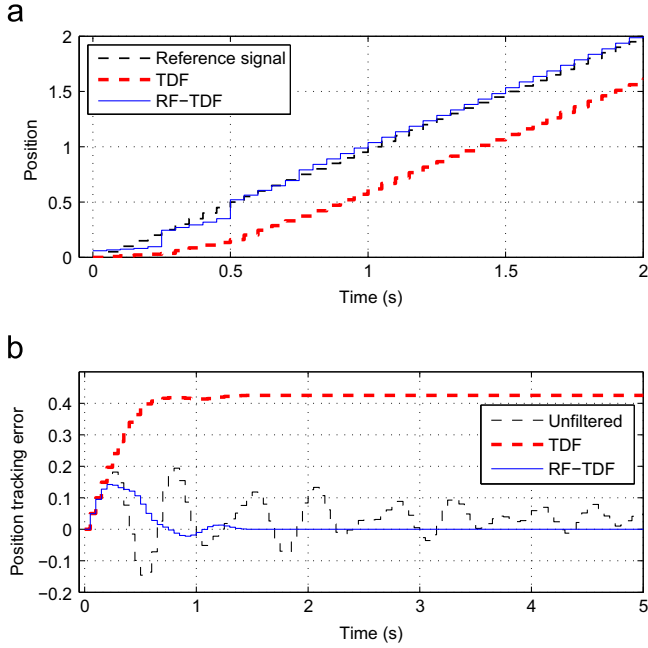


Fig. 11. Discrete system TDF responses for multi-mode systems (sampling time $T_s=0.05$, weighting factor $\lambda=3$). Note that the time axes are scaled differently. (a) Discrete TDF for multiple modes. (b) Reference signal tracking error.

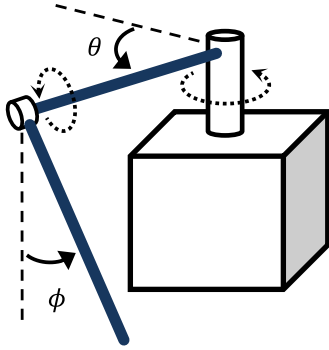


Fig. 12. Schematic of the Quanser rotary pendulum plant with motor arm angle θ and pendulum angle ϕ . The motor arm and the pendulum are considered to be rigid, with lengths L_a and L_p respectively. The stock module has been modified with a slip ring to acquire encoder data from the pendulum while the motor is continuously rotating.

tracking while eliminating residual vibrations. The discrete design of the RF-TDF will follow the same process outlined earlier for the continuous RF-TDF. First consider the stable closed loop transfer function of the form

$$G(z) = \frac{b_m z^m + b_{m-1} z^{m-1} + \dots + b_1 z + b_0}{z^n + a_{n-1} z^{n-1} + \dots + a_1 z + a_0} \quad (29)$$

where $m < n$. Again, assume the DC gain to be unity to obtain the constraint:

$$1 + \sum_{i=0}^{n-1} a_i - \sum_{i=0}^m b_i = 0. \quad (30)$$

The steady state tracking error of the system $G(z)$ subjected to a ramp input $U(z) = T_s z^{-1} / (1 - z^{-1})^2$ is

$$h_{\text{sys}} = \lim_{z \rightarrow 1} (1 - z^{-1}) U(z) (1 - G(z)) \quad (31)$$

$$h_{\text{sys}} = \lim_{z \rightarrow 1} \frac{T_s (z-1) Q(z) + \left[1 + \sum_{i=0}^{n-1} a_i - \sum_{i=0}^m b_i \right]}{z^n + a_{n-1} z^{n-1} + \dots + a_1 z + a_0}, \quad (32)$$

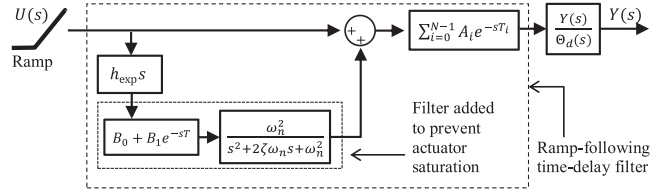


Fig. 13. Experiment block diagram.

where T_s is the sampling time, and

$$Q(z) = z^{n-1} + \sum_{k=2}^{m+1} \left[1 + \sum_{i=1}^{k-1} a_{n-i} \right] z^{n-k} \quad (33)$$

$$+ \sum_{k=1}^m \left[1 + \left(\sum_{j=1}^m a_{n-j} \right) + \sum_{i=1}^k (a_{m-i+1} - b_{m-i+1}) \right] z^{m-k}. \quad (34)$$

Applying (30) to Eq. (32), the ramp tracking error due to the system dynamics reduces to

$$h_{\text{sys}} = \frac{T_s \left(n + \sum_{i=1}^{n-1} i a_i - \sum_{i=1}^m i b_i \right)}{1 + \sum_{i=0}^{n-1} a_i} \quad (35)$$

To account for the time-delay filter $P(z) = \sum_{i=0}^k c_i z^{-i}$, the b terms in $Q(z)$ are multiplied by $P(z)$ and the remainder in (32) becomes $\left[1 + \sum_{i=0}^{n-1} a_i - P(z) \sum_{i=0}^m b_i \right]$. In a process analogous to the continuous-time case, the steady state error due to the TDF becomes

$$h_{\text{tdf}} = T_s \sum_{i=0}^k i c_i \quad (36)$$

Hence the overall steady state ramp tracking error is

$$h = h_{\text{sys}} + h_{\text{tdf}} \quad (37)$$

for the discrete system. Again, the discrete RF-TDF shown in Fig. 6 is completely analogous to its continuous counterpart and no elaboration is necessary. The parameters for $P(z)$ are the solutions to the linear programming problem in (13).

While the derivative element $(z-1)/T_s$ in Fig. 6 in its present form appears to require future knowledge, it can be made causal by multiplying a unit shift z^{-1} . The resulting RF-TDF will maintain the same ramp-following characteristics with this modification, with the final maneuver time delayed by one sampling period.

4. Performance metrics

For the purpose of this paper, the settling time is defined as the time required for a second order system, subject to a unit ramp input in the position, to reach within 5% of the desired velocity. Since the system is simulated numerically, the settling time is subject to the time step used. A small value of $\Delta t = 0.001$ is used for the continuous domain designs in this paper to obtain fairly representative values that can be used to characterize and compare the performance of various input shapers.

Another performance measure for the input shapers is the average tracking error, defined here as

$$\frac{1}{t_f - t_0} \sqrt{\int_{t_0}^{t_f} \left((y(t) - y_{\text{ref}}(t)) \right)^2 dt} \quad (38)$$

where t_0 and t_f are the initial and final time respectively, with y_{ref} being the reference input.

The robustness of the ramp following time-delay filters can be quantified by using the residual energy of the system response

with respect to a frame moving with the reference position, evaluated immediately after the final maneuver:

$$\frac{1}{2} m(\dot{y}_{tf} - \dot{y}_{ref,tf})^2 + \frac{1}{2} k(y_{tf} - y_{ref,tf})^2 \quad (39)$$

where $\dot{y}_{ref,tf}$ is the reference velocity and \dot{y}_{tf} is the velocity of the system following the final maneuver time. Likewise, y_{tf} and $y_{ref,tf}$ denote the final positions. The sensitivities of the input shapers are obtained by simulating the system in (1) across a range of uncertainty in natural frequency, while assuming a normalized mass of $m=1$ and the corresponding stiffness of $k = \omega^2$.

5. Discussion

Kamel et al. (2008) proposed an input shaping technique with control error minimization for low frequency sampled systems, this is different from their approach discussed earlier at the end of Section 3. This input shaper design has been discretized such that the phase lag

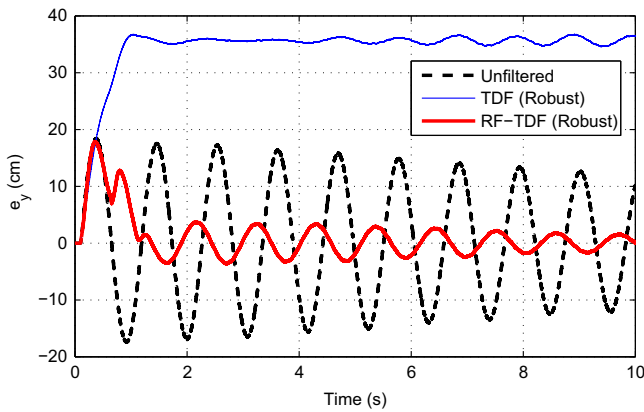


Fig. 14. Representative total displacement error from the experiment.

to a ramp input is a multiple of the sampling period, allowing a predictive path generator to shift the modified input backwards in time. Their method has precise ramp following capabilities, and will be referred to as the control error minimized input shaper (CEM-IS) to serve as a basis of comparison for the design of RF-TDF in this paper.

5.1. Ramp signal

A second order system parameterized by (1) is simulated for a unit ramp in continuous-time with various input shaping schemes. Fig. 7a illustrates the reference input and shaped reference profiles. The displacement jumps in the RF-TDF's require large step inputs, which may lead to actuator saturation; this issue will be addressed in Section 6.

Performance-wise, Fig. 7b shows that the RF-TDF's are able to match the original signal at steady state without the use of backwards time shift employed by CEM-IS. Table 1 shows that RF-TDF's achieve shorter settling times than CEM-IS when predictive path scheduling is not applicable. This is significant since the input ramp signal may be unanticipated in practice. The same table also shows that the non-robust RF-TDF has a smaller settling time than the robust RF-TDF, as expected. Fig. 8 demonstrates that the minimax design based on the classic TDF cost function in (6) is clearly not ideal when precise ramp tracking is required, as the bias in phase persists across the region of uncertainty.

5.2. Finite rate signal

To illustrate the average tracking performance of the proposed input shaper, a complex tracking profile with various ramp segments is taken from Kamel et al. (2008) to benchmark the performance of different input shapers. Fig. 9a illustrates the reference and the shaped input profiles and Fig. 9b shows the corresponding evolution of the tracking error of the second order system. Table 2 lists the root mean square tracking error which shows that non-robust and robust RF-TDF techniques presented in this paper outperformed the traditional robust

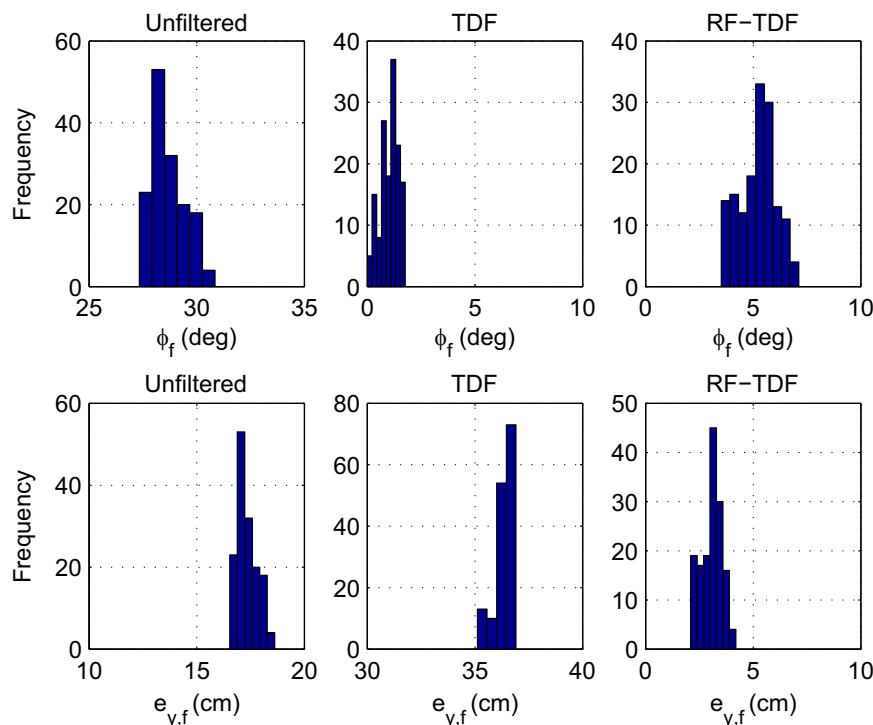


Fig. 15. Residual amplitude histograms from the experiment. For the top plot, the mean values for unshaped input, TDF, and RF-TDF are 28.7°, 1.05°, and 5.21°, respectively. For the bottom plot, the mean values are 0.173, 0.364, and 0.0307 m, in the same order.

TDF, while comparable to the CEM-IS scheme presented by Kamel et al. (2008), which requires backwards time shifting to achieve the precise ramp tracking capability.

5.3. Multi-mode and discrete system

To explore the suitability of the RF-TDF to multi-mode systems, the following system is simulated:

$$G(s) = \frac{s^2 + 2.4s + 22.500}{s^4 + 1.3s^3 + 325.3s^2 + 255s + 22.500} \quad (40)$$

Fig. 10 shows that the RF-TDF successfully eliminates residual vibrations while maintaining steady state zero ramp tracking error. A closer examination of the signal plot shows that the shaped ramp is slightly leading the original ramp signal at steady state – such as to compensate for the h_{sys} term that may have been negligible in the ramp simulations for single mode systems.

The multi-mode system above is discretized with zero-order hold and sampling time $T_s = 0.05$ s. Similar to the continuous-time case, Fig. 11 shows that the RF-TDF designed in the discrete domain also yields perfect tracking with zero residual vibrations for this multi-mode discrete system.

The numerical simulation results are encouraging, as ramp following time-delay filters successfully track ramp commands with zero vibration and zero phase delay, particular when the nominal parameters are known exactly. The RF-TDFs are also shown to be comparable to CEM-IS in terms of the average tracking performance, without requiring a priori knowledge of the signal timing.

6. Experiment

The ramp-following time-delay filter is tested on a Quanser ROTPEN-E rotary pendulum, with schematics shown in Fig. 12. The module has a closed loop PD position controller at the motor arm θ . The linearized model corresponding to the motor arm angle θ and the pendulum angle ϕ is identified, and their transfer functions are given by

$$\frac{\Theta(s)}{\Theta_d(s)} = \frac{1959s^2 + 343.7s + 80.105}{s^4 + 16.15s^3 + 2018s^2 + 943.4s + 80.105} \quad (41)$$

$$\frac{\Phi(s)}{\Theta_d(s)} = \frac{-0.2817s^2(s + 5761)}{s^4 + 16.15s^3 + 2018s^2 + 943.4s + 80.105} \quad (42)$$

with reference motor arm angle θ_d as the input. Note that the PD controller is a part of the identified system.

The objective is for the pendulum tip to track a constant velocity profile in the θ plane, while eliminating any vibrations introduced by the PD control and the pendulum. To evaluate the overall tracking capability, consider the pendulum tip displacement which can be quantified by the equation:

$$y = L_a\theta + L_p\phi, \quad (43)$$

where L_a and L_p are the lengths of the motor arm and the pendulum respectively. To assess the repeatability of the RF-TDF in ramp tracking capability, as well as its sensitivity to the linearized model, the response data for the shaped ramp input is collected for 150 runs. Each run starts from a random initial arm position drawn from a uniform distribution between $\pm 180^\circ$, such that the model inaccuracies can be captured. The same experiment is repeated for the traditional TDF and unfiltered input for comparison. The sampling period is $T_s = 0.0001$ s.

Since errors in the experimentally identified linearized models (41) and (42) are expected, the steady state ramp tracking error for this system, h_{exp} (Fig. 13), should also be determined empirically.

This is accomplished by comparing the reference ramp signal to the system response due to traditional TDF.

In any PD controlled system subjected to step input, the derivative action of the compensator initially demands a large control signal, saturating the actuator. To alleviate this issue, a separate second order filter is cascaded with its own time delay filter to limit the input jerk (As shown in Fig. 13). The parameters of this filter (ζ and ω_n) are arbitrary and are tuned to satisfy the actuator constraint in minimal time; the associated TDF is designed correspondingly based on earlier discussions. The solid line in Fig. 2 is representative of step responses to this type of smoothing filter. This alternative usage of time-delay filter is in the same spirit as the sinusoid filtered time-delay filter in Singh (2010), and adopted here for its simplicity and compatibility with the presented framework.

A representative response for the total displacement error, $e_y = y_d - y$, is shown in Fig. 14, where y_d is the reference ramp input. Note that the closed loop PD motor/arm response is much faster than the pendulum, therefore its dynamics barely manifests in the responses.

Fig. 15 shows the histograms of the residual amplitudes from the experiments. The residual amplitude is defined as the first amplitude peak of the error response of the pendulum, after the final maneuver time of the RF-TDF. In terms of the residual vibration of the pendulum ϕ_f , TDF output marginally outperforms RF-TDF, with 96% vs 82% amplitude reduction. This metric only captures the vibratory motion of the pendulum. When the ramp tracking capability is considered, the total displacement error amplitude $e_{y,f}$ shows that RF-TDF is consistently closer to zero than either the unfiltered or the TDF case. This is due to the fact that the TDF generates a large steady-state tracking error.

7. Conclusions

A simple technique that combines a shaped ramp input with a shaped step input is proposed to achieve zero phase tracking of a ramp profile. This technique has been illustrated in the continuous and discrete time and the results have been compared to existing techniques in the literature. The nature of its closed form solution allows for efficient synthesis and testing of ramp following input shapers/time-delay filters for desired applications. The scheme has been implemented experimentally and shown to be a viable option when vibration reduction with precise ramp tracking capabilities are required specifications.

References

- Butler, H. (2013). Adaptive feedforward for a wafer stage in a lithographic tool. *IEEE Transactions on Control Systems Technology*, 21(3).
- Butterworth, J. A., Pao, L. Y., & Abramovitch, D. (2008). The Effect of nonminimum-phase zero locations on the performance of feedforward model-inverse control techniques in discrete-time systems. In *Proceedings of American control conference*, Seattle, WA, June 11–13.
- Croft, D., & Devasia, S. (1999). Vibration compensation for high speed scanning tunneling microscopy. *Review of Scientific Instruments*, 70(12).
- Devasia, S., Chen, Degang, & Paden, B. (1996). Nonlinear inversion-based output tracking. *IEEE Transactions on Automatic Control*, 41(7), 930–942.
- Kamel, A., Lange, F., & Hirzinger, G. (2008). New aspects of input shaping control to damp oscillations of a compliant force sensor. In *IEEE international conference on robotics and automation*, Pasadena, CA.
- Masterson, R. A., Singhose, W. E., & Seering, W. P. (2000). Setpoint generation for constant-velocity motion of space-based scanners. *AIAA Journal of Guidance, Control, and Dynamics*, 23, 892–895.
- Mathur, P. D., & Messner, W. C. (1998). Controller development for a prototype high-speed low-tension tape transport. *IEEE Transactions on Control Systems Technology*, 6(4).
- Piazzini, A., & Visioli, A. (2002). Optimal dynamic-inversion-based control of an overhead crane. *IEE Proceedings—Control Theory and Applications*, 149(5), 405–411.

- Piazzoli, A., & Visioli, A. (2011). End-point control of a flexible-link via optimal dynamic inversion. In *Advanced intelligent mechatronics, 2001. Proceedings. 2001 IEEE/ASME, Como, Italy*.
- Rhim, S., & Book, W. (2004). Adaptive time-delay command shaping filter for flexible manipulator control. *IEEE/ASME Transactions on Mechatronics*, 9, 619–626.
- Singer, N. C., & Seering, W. P. (1990). Preshaping command inputs to reduce system vibrations. *ASME Journal of Dynamic Systems, Measurement, and Control*, 112, 76–82.
- Singh, T. (2002). Minimax design of robust controllers for flexible systems. *AIAA Journal of Guidance, Control, and Dynamics*, 24(5), 868–875.
- Singh, T. (2010). *Optimal reference shaping for dynamical systems*. Boca Raton, FL: CRC Press.
- Singh, T., & Vadali, S. R. (1993a). Input-shaped control of three-dimensional maneuvers of flexible spacecraft. *AIAA Journal of Guidance, Control, and Dynamics*, 16(6), 1061–1068.
- Singh, T., & Vadali, S. R. (1993b). Robust time-delay control. *ASME Journal of Dynamic Systems, Measurement, and Control*, 115, 303–306.
- Smith, O. J. M. (1957). Postcast control of damped oscillatory systems. In *Proceedings of the IRE* (pp. 1249–1255).
- Sorensen, K., Singhose, W., & Dickerson, S. (2007). A controller enabling precise positioning and sway reduction in bridge and gantry cranes. *Control Engineering Practice*, 15, 825–837.
- Tomizuka, M. (1987). Zero phase error tracking algorithm for digital control. *ASME Journal of Dynamic Systems, Measurement, and Control*, 109, 65–68.
- Tzes, A., & Yorkovich, S. (1993). An adaptive input shaping control scheme for vibration suppression in slewing flexible structures. *IEEE Transactions on Control Systems Technology*, 1.